Video Article

Full-field Optical Coherence Microscopy for Histology-like Analysis of Stromal Features in Corneal Grafts

Kristina Irsch[1,2,3], Kate Grieve[1,2], Marie Borderie[1], Djida Ghoubay[1,2], Cristina Georgeon[1], Vincent Borderie[1,2]

[1]Quinze Vingts National Ophthalmology Hospital

[2]Vision Institute/CIC 503, UPMC-Sorbonne Universities, UMR_S 968 / INSERM, U968 / CHNO des XV-XX / CNRS, UMR_7210

[3]Laboratory of Ophthalmic Instrument Development, The Wilmer Eye Institute, Johns Hopkins University School of Medicine

Correspondence to: Kristina Irsch at kristina.irsch@gmail.com

URL: https://www.jove.com/video/57104
DOI: doi:10.3791/57104

Keywords: Imaging, cornea, keratoconus, optical coherence tomography, microscopy, donor tissue, keratocyte, stroma, corneal transplantation, corneal storage

Date Published: 11/29/2017

Citation: Irsch, K., Grieve, K., Borderie, M., Ghoubay, D., Georgeon, C., Borderie, V. Full-field Optical Coherence Microscopy for Histology-like Analysis of Stromal Features in Corneal Grafts. *J. Vis. Exp.* (), e57104, doi:10.3791/57104 (2017).

Abstract

The quality of donor corneal stroma, which makes up about 90% of total corneal thickness, is likely to be one of the main, if not the major, limiting factor(s) for success of deep anterior lamellar and penetrating keratoplasty. These are surgical procedures that involve replacing part or all of the diseased corneal layers, respectively, by donated tissue, the graft, taken from a recently deceased individual. However, means to evaluate stromal quality of corneal grafts in eye banks are limited and lack the capability of high-resolution quantitative assessment of disease indicators. Full-field optical coherence microscopy (FF-OCM), permitting high-resolution 3D imaging of fresh or fixed *ex vivo* biological tissue samples, is a non-invasive technique well suited for donor cornea assessment. Here we describe a method for the qualitative and quantitative analysis of corneal stroma using FF-OCM. The protocol has been successfully applied to normal donor corneas and pathological corneal buttons, and can be used to identify healthy and pathologic features on both the macroscopic and microscopic level, thereby facilitating the detection of stromal disorders that could compromise the outcome of keratoplasty. By improving the graft quality control, this protocol has the potential to result in better selection (and rejection) of donor tissues and hence decreased graft failure.

Introduction

Corneal diseases are amongst the major causes of blindness worldwide[1]. Some diseases can only be treated surgically, often involving the replacement of part (*i.e.*, lamellar keratoplasty) or the entire (*i.e.*, penetrating keratoplasty) diseased cornea, by donated tissue, the graft, taken from a recently deceased individual. For corneal diseases that do not affect the endothelium (*e.g.*, keratoconus, stromal scars after infectious keratitis, trauma, and stromal dystrophies), deep anterior lamellar keratoplasty (DALK) is currently considered as the surgical technique of choice[2,3,4,5]. This technique makes possible the preservation of the recipient's corneal endothelium, by replacing only the central corneal epithelium and stroma, which is associated with a lower incidence of graft rejection, absence of endothelial rejection, lower endothelial cell loss, and favorable cost-effectiveness ratio[6,7,8,9,10,11]. DALK further allows corneas with less than optimal endothelium quality to be used as grafts, as this compromised layer will not be transplanted[12]. Conversely, quality of donor corneal stroma is likely to be the major limiting factor for graft success and vision recovery because the stroma is the only donor corneal layer to remain, while the donor epithelium will be replaced by recipient epithelium. Unfortunately, means to assess donor corneal stroma in eye banks are limited. They usually include slit-lamp examination of the donor eyeball when tissue retrieval is made by enucleation and light microscope examination of the donor stroma[13]. Some eye banks have started supplementing such standard procedures using Fourier-domain optical coherence tomography (FD-OCT)[14].

Ophthalmic optical coherence tomography (OCT), an optical analogue to ultrasound imaging[15], uses interference of broadband or tunable light to generate optical sections of the retina[16] and anterior segment[17]. In time-domain OCT, the basis of early clinical systems, the position of a reference mirror is altered, so that interference patterns show up whenever the reference beam has traveled almost the same amount of time as the beam reflected at the various tissue interfaces, with A-scans being generated as a function of time. In FD-OCT (also called spectral- or frequency-domain OCT), the basis of most modern clinical systems, the reference mirror is fixed at one position and an individual A-scan, with all interference patterns mixed together, is acquired at a time, and dissected apart via Fourier analysis.

While clinical (time or spectral-domain) OCT systems permit cross-sectional views of the cornea and the detection of stromal opacities at a higher axial resolution than slit-lamp biomicroscopy, their lateral resolution is limited. Confocal microscopy[18] allows examination of the cornea at a lateral resolution approaching histological detail, but is limited axially.

Full-field optical coherence tomographic microscopy (FF-OCT or FF-OCM)[19,20] combines elements of both confocal microscopy and OCT, achieving a lateral resolution comparable to the axial resolution of about 1 µm. More specifically, FF-OCM uses incoherent broadband light sources (*e.g.*, a halogen lamp) and high numerical aperture optics to acquire *en face* 2D tomographic images without lateral scanning. By scanning in the depth direction, FF-OCM enables non-invasive 3D imaging of fresh or fixed *ex vivo* biological tissue samples. It has been used to image the cornea[21,22,23]. By providing both high-resolution *en face* and cross-sectional views, FF-OCM provides information on both the

histological structure and cellular details of the cornea. In fact, FF-OCM has been shown to provide structural information superior to histology and was able to identify more disease indicators as was possible with the combination of spectral-domain OCT and confocal microscopy[24,25].

Here we describe a protocol for the qualitative and quantitative assessment of corneal donor stroma using FF-OCM. The method is based on the histology-like analysis of macroscopic and microscopic features indicative of stromal condition, including three quantitative stromal parameters (*i.e.*, Bowman's layer thickness and its variability, and stromal reflectivity). The described protocol is therefore applied to normal and abnormal cornea tissues and permits differentiation of diseased from normal human corneal tissues.

Protocol

All methods described here were carried out according to the tenets of the Declaration of Helsinki and followed international ethical requirements for human tissues. This was a prospective observational case control study. Informed consent was obtained from patients. No modifications to French standards of treatment or follow-up were made. Institutional Review Board (IRB) approval was obtained from the Patient Protection Committee, Ile-de-France V (14944).

1. Tissue Selection and Preparation

1. **Select donor corneas.**
    1. Transfer donor corneas stored in organ culture medium[26] to dextran-supplemented organ culture medium for 3 days to allow deturgescence[27] prior to FF-OCM imaging[28] (see **Table of Materials**).

2. **Prepare the samples.**
    1. Position the cornea, immersed in storage medium, in the sample holder with the epithelium facing up.
    2. Place a clean silica coverslip (provided with the sample holder) on top of the cornea and close the holder by gently turning its base until the sample is slightly flattened and immobilized under the coverslip providing a relatively even imaging surface. Take precautions to avoid any air bubbles.
    3. Apply a thick layer of ophthalmic or optical gel on the coverslip as the immersion medium.

2. FF-OCM Initialization, Setup, and Image Acquisition

1. **Initialize the device.**
    1. Turn on the device by operating the power switch on the back of the device; illumination of a green LED on the front of the device indicates that the power is on.
    2. Turn on the dedicated computer and halogen light source by operating the power switch on the front.
    3. Launch the acquisition software (see **Table of Materials**) by double-clicking on the desktop shortcut.
    4. Ensure that the imaging stage is clear except for the movable tray. Then click "OK" to initialize the motors at the prompt.
    5. Pull out the tray and insert the sample holder in the dedicated container, then gently push back the tray.

2. **Setup the device.**
    1. Enter a "sample identifier" in the designated and mandatory field; optionally enter a "sample description" and/or "study description".
    2. Click "Acquire macro image" when ready, to create a snapshot of the sample that can be used for lateral positioning and navigation purposes later; once satisfied, validate the image at the prompt by clicking "Yes", after which the device moves the sample tray underneath the objective and performs an auto-adjustment.
    3. Ensure that the microscope objective is well immersed in the optical gel before proceeding further.

3. **Acquire the stacks.**
    1. **Select the "Explore" tab to prepare an acquisition.**
        1. Before acquiring a stack of images, navigate to the center of the cornea, via translation of the joystick or manual selection on the screen (that is, by clicking and dragging the red square on the acquired macro image to the desired location).
        2. Vary the imaging depth via rotation of the joystick, adjustment of the slider, or manual keyboard input in the graphical user interface (GUI), and adjust the averaging value (an averaging of 40 is generally recommended for optimal corneal imaging). NOTE: This is done to determine the thickness of the corneal sample and the averaging necessary to image through the entire corneal thickness while noting the first and last image location in depth. The bottom surface of the coverslip creates parallel interference fringes that are seen on the tomographic image (on the right-hand side of the GUI), which facilitate locating the corneal surface.
        3. Enter the corneal surface value or first image location in depth into the "Depth" field.

    2. **Select the "Acquire tab", to acquire images.**
        1. Select the "Slice spacing" (the default and recommended setting is 1 µm, matching the axial resolution of the device) and enter the corneal thickness value accordingly, under "Number of slices".
        2. Review parameters and acquisition time, and when satisfied press "OK" to launch the acquisition.
        3. During the acquisition, avoid any contact with the table on which the FF-OCM is positioned.

3. Management of Acquired Images

1. **View and export images.**
    1. Launch the FF-OCM viewing software (see **Table of Materials**) by double-clicking on the desktop shortcut; acquired images (identified by the sample ID) appear in the "Local Studies" list.
    2. Select the study with corresponding sample ID, which contains both the macro image and acquired image stack, and "export" the latter by right-clicking on the series of images and selecting the "DICOM" format to retain the raw pixel data and metadata for further analysis.
    3. Display the 3D image stacks in *en face* and cross-sectional views using the multiplanar reconstruction (MPR) mode, by double-clicking on the series of images; navigate through the images (*e.g.*, via mouse-wheel scroll or slider adjustment) and select representative *en face* and cross-sectional views of each stack.
    4. Export the selected views by clicking on the icon at the bottom right of the window, using the "DICOM" format.

2. **Import images.**
    1. Open the image processing software (see **Table of Materials**) by double-clicking on the desktop shortcut, and navigate to the "Bio-Formats" "Importer" under "Plugins" to import DICOM images; make sure that "Group files with similar names" is selected in the "Bio-Formats Import Options" window.

4. Image Analysis: Qualitatively and Quantitatively Assessment of Stromal Morphology and Features

1. **Assess stromal and Bowman's layer thickness.**
    1. Measure distances manually on corneal cross-sections, for example at five equally spaced points across the cross-section[25].
        1. Draw a line between two points of known distance (such as, from left to right of the entire image, that is according to the default field-of-view, 1,024 pixels or 780 µm), go to "Analyze" and select "Set Scale", and enter the "Known distance" and "Unit of length" in the appropriate fields and click "OK".
        2. Draw a line between two points of unknown distance; read the length or distance measured directly from the status bar.

    2. Record the mean and coefficient of variation (COV). Bowman's layer thickness less than 6.5 µm and a COV greater than 18.6% have been associated with abnormal corneal stroma[25].

2. **Determine the keratocyte density.**
    1. Following convention of confocal microscopy: sum stromal *en face* images in groups of 7 to produce slices of comparable thickness. For this, go to the "Image" tab and select "Reslice Z" under "Stacks".
    2. Take into account the differing (decreasing) cell density on progression through the stroma[24,25]. For this, the stroma may be considered as being composed of 4 regions according to depth: (1) the very anterior stroma below Bowman's layer, that is 2% of entire stromal thickness; the remaining stroma (that is, 98% of entire stromal thickness), with three zones of identical thickness: (2) anterior stroma, (3) mid stroma, and (4) posterior stroma.
    3. For further analysis, include all available *en face* slices for the very anterior stroma, 15 images for the anterior stroma, 5 images for the mid stroma, as well as 5 images for the posterior stroma (where the number of images per region required for a reliable count was determined by stepwise analysis[29]).
    4. On each *en face* image, select a 300 µm x 300 µm region of interest. To enhance nucleus visualization, invert the image, using "Invert" under the "Edit" tab, and adjust contrast and brightness. For the latter, go to "Image" and navigate to "Brightness/Contrast" under "Analyze".
    5. Manually count cell nuclei, using for example the "cell counter" function[25]. For this, go to "Plugins" and navigate to "Cell Counter" under "Analyze". Select a counter type and then press "Initialize". Then start counting the cell nuclei by clicking on dark oval features in the inverted image, considering those landing on an image border only for two of the four sides of the image[25].
    6. Record the cell density in terms of area density, that is in cells/mm² (multiply the number of cells counted by 0.09, to convert from cells/90,000 µm² to cells/mm²), following confocal microscopy convention where keratocyte densities have been shown to be lower in patients (*e.g.*, with keratoconus) than in healthy subjects and to be correlated with disease severity[25].
    NOTE: Further clinical studies are necessary to determine whether a minimal threshold of keratocyte density is required to obtain a perfectly clear corneal graft after transplantation.

3. **Assess the stromal reflectivity.**
    1. Generate mean intensity depth profiles of stromal image stacks, using for example the "Z-axis profile" function and/or custom software[30,25].
        1. Calculate the mean grey level for each *en face* stack.
        2. Subtract the minimum grey value and normalize by the maximum grey value.
        3. Display in log scale as a function of stromal depth (% of the stromal thickness).
        4. Approximate the resulting logarithmic profile by a linear regression line, which minimizes the sum of the squared residuals (least-squares fit).
        5. Record the R-square value (R^2) as a measure of linearity. Values below 0.94 could be an indication of corneal pathology[25].

4. **Assess the visibility of other stromal features and disease indicators.**
    1. Check for the presence of scars, fibrotic tissue, lakes, or Vogt striae.
    2. Assess mean thickness of nerves in the stroma, if sufficiently visible for measurement[24].
        1. Select one *en face* image where the stromal nerve is most visible (generally in the mid-stromal region).

2. Measure the thickness of the nerve, for example at five points[24], then calculate the mean and standard deviation. Nerve thicknesses above 9 µm may be an additional indicator for pathology, such as keratoconus[24].

Representative Results

The FF-OCM device (see **Table of Materials**)[28] and general setup used in this manuscript is shown in **Figure 1**. **Figure 2** shows a swelled human donor cornea after storage in organ culture medium, giving a pathophysiological model of edematous cornea and preventing FF-OCM image acquisition through the entire corneal thickness due to limited penetration depth. Transfer to dextran-supplemented organ culture medium causes deswelling and results in donor corneas of normal thickness, as represented in **Figure 3**. Diseased corneas can be recognized by morphological changes and typical stromal features, including a decreased and variable thickness of the stroma (**Figure 4**) and/or Bowman's layer (**Figure 5**). Assessment of the keratocyte density (**Figure 6**) and stromal reflectivity (**Figure 7**) may further aid in the histology-like analysis and differentiation of normal from pathologic corneal tissues with FF-OCM, beyond the capabilities of clinical OCT systems (**Figure 8**).

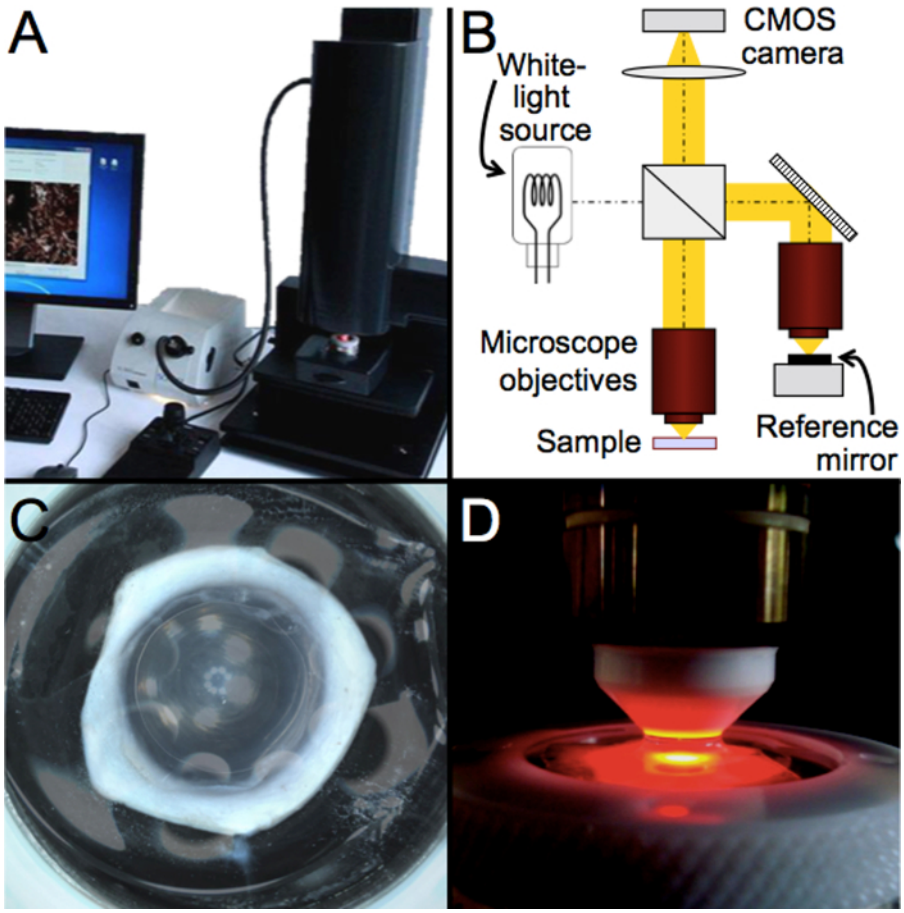

Figure 1: Schematic and photographs of the general setup and FF-OCM device used in this work. (**A**) Photograph of the FF-OCM device (see **Table of Materials**)[28]. (**B**) Schematic and optical setup of the device. (**C**) Photograph of a human donor cornea in the sample holder. (**D**) Zoom on the immersion objective and the sample holder. Please click here to view a larger version of this figure.

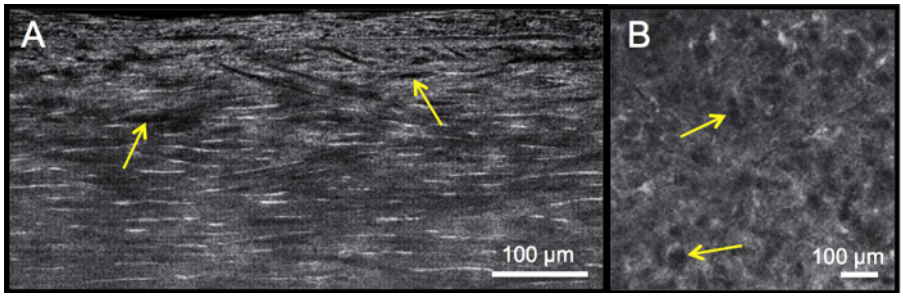

Figure 2: Organ-cultured normal human cornea before deturgescence. Cross-sectional (**A**) and *en face* view (**B**, slice through the stroma) of swelled ("edematous") cornea caused by storage in organ culture medium, where lakes can be seen as dark areas (as indicated by arrows). Corneal thickness has doubled to over 1,100 µm, preventing image acquisition through the entire depth. Please click here to view a larger version of this figure.

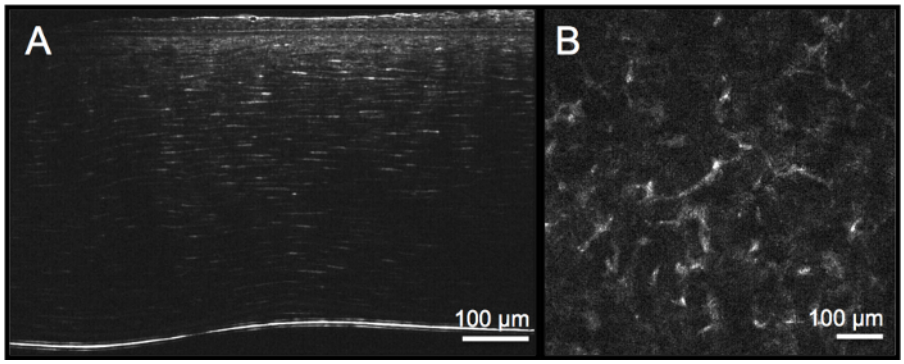

Figure 3: Organ-cultured normal human cornea after deturgescence. Cross-sectional view through the entire cornea (**A**) and *en face* stromal view (**B**) of de-swelled cornea immersed in dextran-supplemented medium, showing regularly distributed hyper-reflective (white) keratocytes. Please click here to view a larger version of this figure.

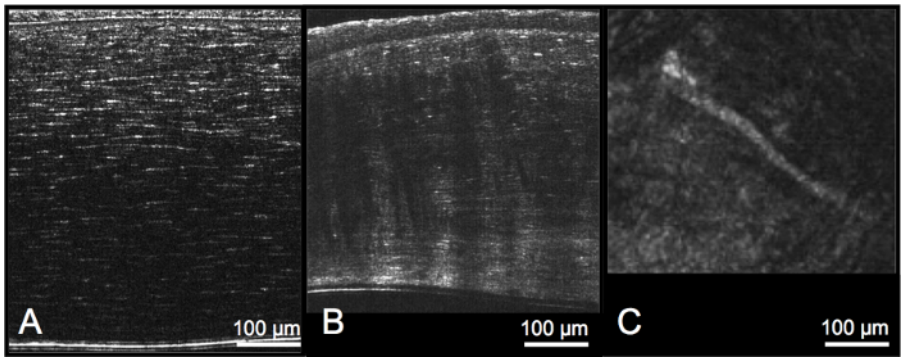

Figure 4: Overall assessment of stromal morphology and features, including stromal thickness. Compared with normal human cornea (**A**), corneas with keratoconus (**B**) feature decreased and variable stromal thickness, along with numerous, parallel Vogt striae that are observable as dark vertical bands in cross-sectional views, and thick stromal nerves that may be found in mid-stromal *en face* slices (**C**). Please click here to view a larger version of this figure.

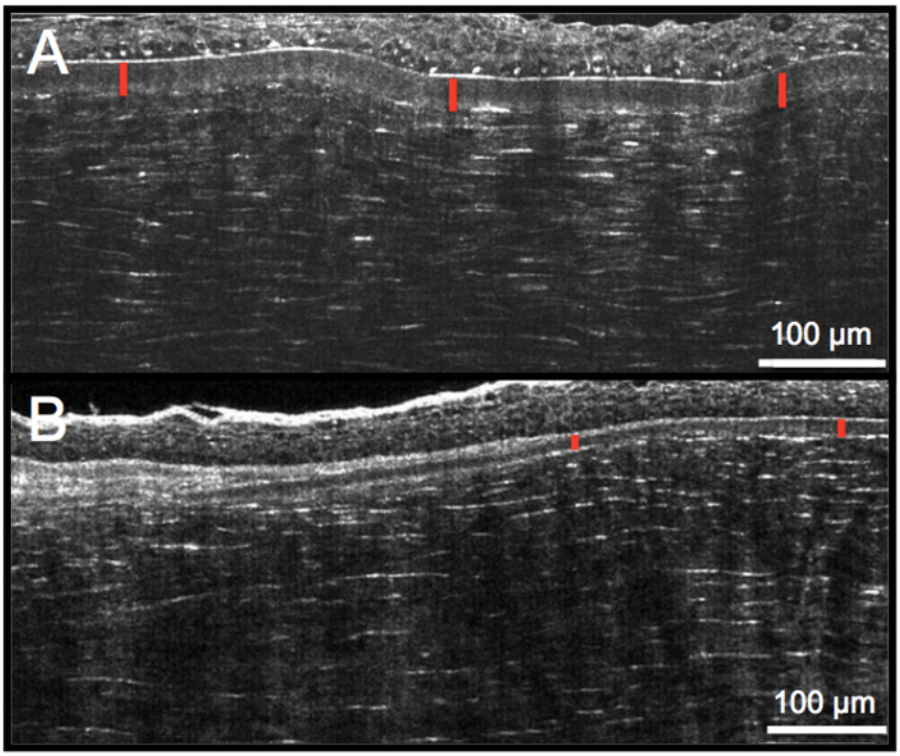

Figure 5: Assessment of Bowman's layer thickness, which is delineated anteriorly by the hyper-reflective epithelial basement membrane and posteriorly by the hyper-reflective keratocytes in the very anterior stroma. Compared with a normal human cornea (**A**), pathologic cornea (*e.g.*, keratoconus) (**B**) features decreased and variable Bowman's layer thickness due to interruption and scarring. Please click here to view a larger version of this figure.

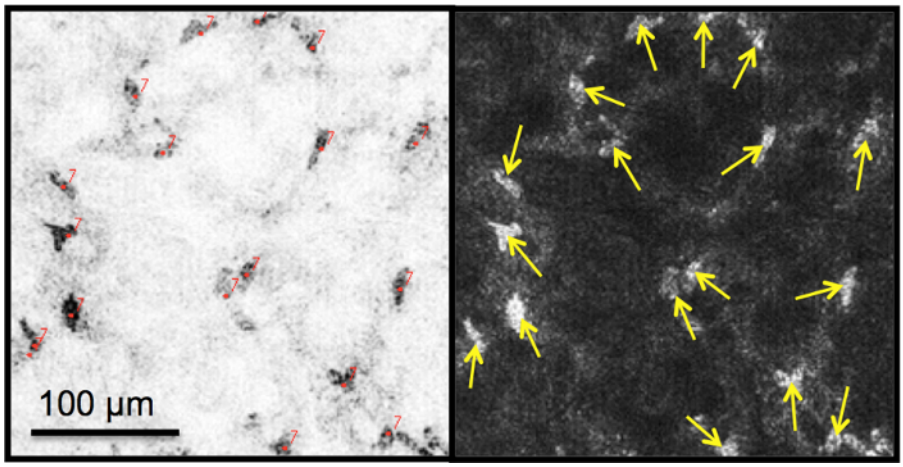

Figure 6: Assessment of keratocyte density. (**A**) Keratocyte nuclei are manually counted on enhanced and inverted *en face* images after selection of a 300 µm x 300 µm region of interest. (**B**) Counted nuclei are indicated by arrows. Please click here to view a larger version of this figure.

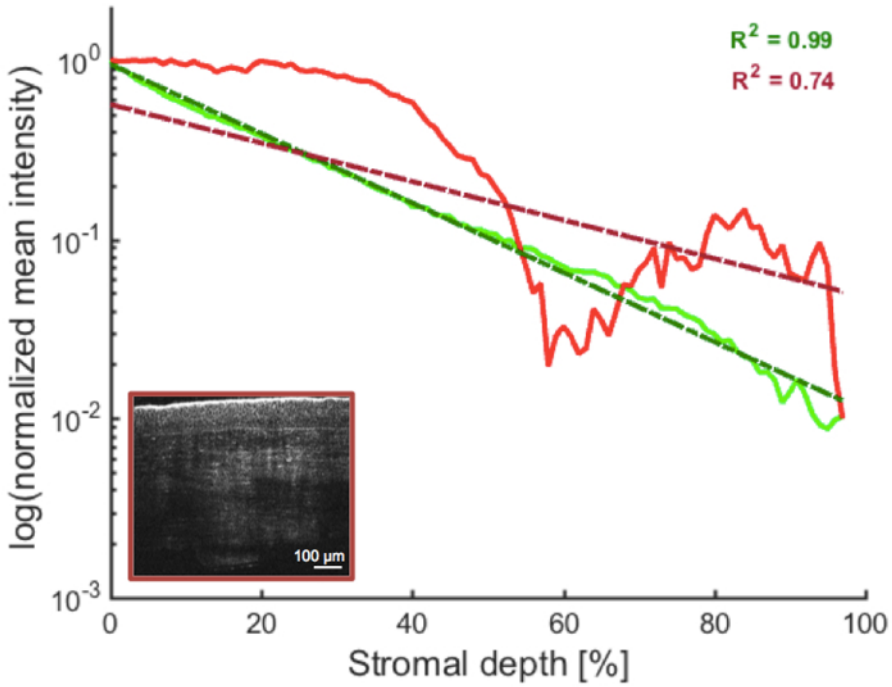

Figure 7: Assessment of stromal reflectivity. The intensity of backscattered light decreases (exponentially) with depth in the stroma of normal donor corneas (see **Figure 3** and **Figure 4A**), resulting in linear logarithmic depth profiles, represented by R-square values close to 1 (green trace). This may not hold true for pathological corneas featuring stromal regions of increased light backscatter (see **Figure 4B**). The presence of such macroscopic features, as in the example of a cornea with stromal scar after infectious keratitis (depicted in the inset), will thus create non-linear logarithmic intensity depth profiles, represented by an R-square value lower than 0.94[25] (red trace). Please click here to view a larger version of this figure.

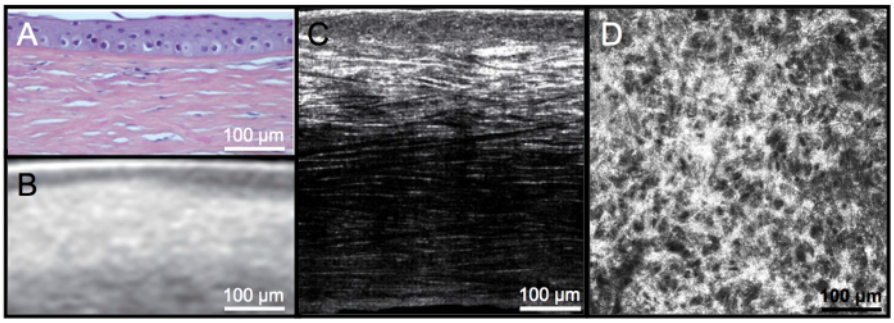

Figure 8: Demonstration of benefits of FF-OCM over histology and spectral-domain OCT. (**A**) Histology and (**B**) corresponding spectral-domain-OCT image acquired on the same cornea *in vivo* prior to keratoplasty. (**C**) Corresponding FF-OCM cross section of the *ex vivo* corneal button post-keratoplasty, illustrating superior resolution compared to the clinical spectral-domain OCT images. The fibrosis is also more clearly visible in FF-OCM images than in the histology. The high density of keratocytes in the upper stroma can clearly be seen in both the (**C**) cross-sectional and (**D**) *en face* views. Please click here to view a larger version of this figure.

Discussion

The protocol described here for the qualitative and quantitative assessment of corneal donor stroma using FF-OCM is based on the histology-like analysis of macroscopic and microscopic features indicative of stromal condition, beyond the capabilities of spectral-domain OCT and confocal microscopy[21,24,25], and enables differentiation of diseased from normal human tissues.

Aside from an excellent endothelial quality assessment of human donor corneas by means of specular microscopy, assessment of stromal quality is challenging in eye banks, and generally limited to a gross observation with slit-lamp biomicroscopy and/or light microscopy in current protocols. Lack of fine resolution with existing methods not only means that corneas with some stromal disease may be selected that compromise the result of keratoplasty, but also that corneas may be rejected for stromal opacities that are in fact constraint to anterior stroma or epithelial regions and could still be used for endothelial keratoplasty procedures[14].

The current eye-bank protocol could be supplemented by the addition of FF-OCM, which due to its superior resolution, constitutes a powerful and non-invasive tool to complete the quality assessment of the cornea, especially the stroma (including Bowman's layer). Unlike during slit-lamp

examination, the graft remains immersed in a closed chamber filled with storage medium throughout FF-OCM image acquisition, decreasing any potential risk of contamination.

For successful image acquisition with FF-OCM (see **Table of Materials**), it is important for the microscope objective to be well immersed in the optical gel that is applied on top of the coverslip of the sample holder (step 2.2.3). It is further recommended to regularly check the calibration of the device, a procedure also to be performed after unsuccessful auto-adjustment (step 2.2.2) and accessed via "Tools and options" in the acquisition software (see **Table of Materials**). The procedure, which involves the utilization of a calibration mirror in the sample holder, is the same as the usual sample preparation (see step 1.2) except that the optical gel should be applied on the mirror before positioning of the coverslip.

A series of donor corneal grafts, considered to have normal stroma as per existing eye-bank procedures, were used to describe the protocol in this manuscript and specifically demonstrate the suitability of FF-OCM for precise and reliable assessment of donor stromal quality. These normal donor corneas were compared with pathological corneas immersed in storage medium, showing that the histology-like analysis made possible with FF-OCM of several stromal features (illustrated in **Figure 2**, **Figure 3**, **Figure 4**, **Figure 5**, **Figure 6**, **Figure 7**, and **Figure 8**) in corneal grafts allows distinguishing diseased from normal human corneal tissues.

Aside from morphological changes, such as the presence of scars (**Figure 5** and **Figure 7**), fibrotic tissue (**Figure 8**), lakes (**Figure 2**), Vogt striae (**Figure 4**), or increased stromal nerve diameter (**Figure 4**), typical stromal features are present in diseased corneas. Stromal parameters particularly relevant in the stromal quality assessment appear to be Bowman's layer thickness and its variability, and stromal reflectivity. Critical steps within the protocol are thus steps 4.1 and 4.3.

While being secreted during human corneal development, Bowman's layer, in particular, becomes distinct by 19 weeks of gestation and never repairs after birth[31]. Damage to Bowman's layer is thus irreversible and serves as an ideal indicator of previous stromal damage in donor corneal tissue, including damage caused by refractive surgery, infectious keratitis, keratoconus. Such corneal diseases, which constitute contraindications for donor corneal usage, are associated with decreased and variable Bowman's layer thickness due to interruption and scarring (**Figure 5**), and are likely to be missed by current eye-bank protocols when the donor history is not precisely known.

Although corneal transparency is impaired after donor death due to *post mortem* corneal edema, the intensity of backscattered light, or stromal reflectivity is expected to decrease exponentially with depth in the stroma (see **Figure 3** and **Figure 4A**); as a result, the logarithm of normalized stromal reflectivity will be a linear function of stromal depth in normal donor corneas, represented by R-square values close to 1. Conversely, the presence of macroscopic features is associated with non-linear logarithmic intensity depth profiles and indicative of stromal disease (**Figure 4B** and **Figure 7**)[25].

Since keratocyte density is responsible for stromal collagen fibril and extracellular matrix synthesis and renewal, it appears reasonable to assume that keratocyte density is another relevant parameter for assessing donor stromal quality, and that tissues exhibiting very low keratocyte counts should not be transplanted. The protocol therefore includes a precise and reliable method to measure keratocyte density from FF-OCM images that can be easily used in eye banks[25] and follows the convention of confocal microscopy. Note that with FF-OCM, keratocyte density may also be determined by counting keratocytes directly in the cross-sectional view[32], a potential advantage over confocal microscopy, which requires keratocytes to be counted on multiple *en face* slices. However, unlike in living patients, where keratocyte densities have been demonstrated to be lower in disease patients than in normal controls[33,34,35,36] and to correlate with disease severity[33,37], this was not the case in human *ex vivo* tissue samples[25], and further studies are necessary to determine whether a minimal number of keratocytes is required in donor corneas to result in good visual recovery after transplantation. Low keratocyte density in donor tissue as in pathological tissue could be explained by aging, *post mortem* loss of cells induced by ischemia, and/or storage of donor tissue[27,38,39,40]. It should also be pointed out that the normal donor corneas that were obtained and imaged in this protocol were either stored and edematous or de-swelled, or had been discarded by the eye bank before transplantation because of poor endothelial quality according to the standards of the EU Eye Bank Association. Were FF-OCM imaging along with the described protocol to be included in the eye bank setting, the corneas would typically be assessed in a fresher state than was possible here, which may affect the keratocyte densities.

The protocol described here for the stromal quality analysis could be extended for assessment of Descemet's membrane, which can also be resolved with FF-OCM in terms of thickness and structure[21,24]. This may prove useful for selection of tissues for Descemet's membrane endothelial keratoplasty, where thin Descemet's membranes may be more difficult to separate from the stroma.

In conclusion, FF-OCM enables precise and reliable assessment of human donor corneal stroma during storage. By improving the graft quality, the addition of this protocol to current eye-banking procedures has the potential to improve the screening and selecting of donor tissues, and hence the results of keratoplasty. Real-life integration of the FF-OCM device into the eye-bank routine should be facilitated by recent technological updates, including faster image acquisition and larger field of view thanks to the development of a custom CMOS camera, and the design of custom sterile disposable cassettes for cornea storage and handling during imaging.

Disclosures

The authors have nothing to disclose.

Acknowledgements

This work has received funding from the Agence Nationale de Recherche (ANR), under a PRTS (Projet de Recherche Translationelle en Santé) grant No ANR-13-PRTS-0009 (V.B.) and from the European Union's Horizon 2020 research and innovation programme under the Marie Skłodowska-Curie grant agreement No 709104 (K.I.). The authors thank Céline de Sousa for help with cell counting and histological processing.

References

1. Pascolini, D., Mariotti, S.P. Global estimates of visual impairment: 2010. *Br J Ophthalmol.* **96**, 614 - 618 (2012).
2. Shimazaki, J., Shimmura, S., Ishioka, M., Tsubota, K. Randomized clinical trial of deep lamellar keratoplasty vs penetrating keratoplasty. *Am J Ophthalmol.* **134**, 159 - 165 (2002).
3. Tsubota, K., Kaido, M., Monden, Y., Satake, Y., Bissen-Miyajima, H., Shimazaki, J. A new surgical technique for deep lamellar keratoplasty with single running suture adjustment. *Am J Ophthalmol.* **126**, 1 - 8 (1998).
4. Busin, M., Zambianchi, L., Arffa, R.C. Microkeratome-assisted lamellar keratoplasty for the surgical treatment of keratoconus. *Ophthalmology.* **112**, 987 - 997 (2005).
5. Amayem, A.F., Anwar, M. Fluid lamellar keratoplasty in keratoconus. *Ophthalmology.* **107**, 76 - 79 (2000).
6. Borderie, V.M., Guilbert, E., Touzeau, O., Laroche, L. Graft rejection and graft failure after anterior lamellar versus penetrating keratoplasty. *Am J Ophthalmol.*, **151**, 1024 - 1029 (2011).
7. Borderie, V.M., Sandali, O., Bullet, J., Gaujoux, T., Touzeau, O., Laroche, L. Long-term results of deep anterior lamellar versus penetrating keratoplasty. *Ophthalmology.* **119**, 249 - 255 (2012).
8. Koo, T.S., Finkelstein, E., Tan, D., Mehta, J.S. Incremental cost-utility analysis of deep anterior lamellar keratoplasty compared with penetrating keratoplasty for the treatment of keratoconus. *Am J Ophthalmol.* **152**, 40 - 47 (2011).
9. Bahar, I., Kaiserman, I., Srinivasan, S., Ya-Ping, J., Slomovic, A.R., Rootman, D.S. Comparison of three different techniques of corneal transplantation for keratoconus. *Am J Ophthalmol.* **146**, 905 - 912 (2008).
10. Bahar, I., Kaiserman, I., Srinivasan, S., Ya-Ping, J., Slomovic, A.R., Rootman, D.S. Longterm results of deep anterior lamellar keratoplasty for the treatment of keratoconus. *Am J Ophthalmol.* **151**, 760 - 767 (2011).
11. Cheng, Y.Y., *et al*. Endothelial cell loss and visual outcome of deep anterior lamellar keratoplasty versus penetrating keratoplasty: a randomized multicenter clinical trial. *Ophthalmology.* **118**, 302 - 309 (2011).
12. Borderie, V.M., Sandali, O., Bullet, J., Guilbert, E., Goldschmidt, P., Laroche, L. Donor tissue selection for anterior lamellar keratoplasty. *Cornea.* **32**, 1105 - 1109 (2013).
13. Borderie, V., Martinache, C., Sabolic, V., Touzeau, O., Laroche, L. Light microscopic evaluation of human donor corneal stroma during organ culture. *Acta Ophthalmol Scand.* **76**, 154 - 157 (1998).
14. Bald, M.R., Stoeger, C., Galloway, J., Tang, M., Holiman, J., Huang, D. Use of fourier-domain optical coherence tomography to evaluate anterior stromal opacities in donor corneas. *J Ophthalmol.* **2013**, 397680 (2013).
15. Huang, D., *et al.* Optical coherence tomography. *Science.* **254**, 1178-1181 (1991).
16. Swanson, E.A., *et al.* In vivo retinal imaging by optical coherence tomography. *Opt Lett.* **18**, 1864 - 1866 (1993).
17. Izatt, J.A., et al. Micrometer-scale resolution imaging of the anterior eye in vivo with optical coherence tomography. *Arch Ophthalmol.* **112**, 1584 - 1589 (1994).
18. Stave, J., Zinser, G., Grummer, G., Guthoff, R. Modified Heidelberg retinal tomograph HRT. Initial results of in vivo presentation of corneal structures. *Ophthalmologe.* **99**, 276 - 280 (2002).
19. Beaurepaire, E., Boccara, A.C., Lebec, M., Blanchot, L., Saint-Jalmes, H. Full-field optical coherence microscopy. *Opt Lett.* **23**, 244 - 246 (1998).
20. Dubois, A., Vabre, L., Boccara, A.C., Beaurepaire, E. High-resolution full-field optical coherence tomography with a Linnik microscope. *Appl Opt.* **41**, 805 - 812 (2002).
21. Ghouali, W., *et al.* Full-field optical coherence tomography of human donor and pathological corneas. *Curr Eye Res.* **24**, 1 - 9 (2014).
22. Akiba, M., *et al.* Ultrahigh-resolution imaging of human donor cornea using full-field optical coherence tomography. *J Biomed Opt.* **12**, 041202 (2007).
23. Latour, G., Georges, G., Lamoine, L.S., Deumie, C., Conrath, J., Hoffart, L. Human graft cornea and laser incisions imaging with micrometer scale resolution full-field optical coherence tomography. *J Biomed Opt.* **15**, 056006 (2010).
24. Grieve, K., Georgeon, C., Andreiuolo, F., Borderie, M., Ghoubay, D., Rault, J., Borderie, V.M. Imaging microscopic features of keratoconic corneal morphology. *Cornea.* **35**, 1621 - 1630 (2016).
25. Borderie, M., *et al.* New parameters in assessment of human donor corneal stroma. *Acta Ophthalmol.* **95**, e297 - e306 (2017).
26. Borderie, V.M., Scheer, S., Touzeau, O., Vedie, F., Carvajal-Gonzalez, S., Laroche, L. Donor organ cultured corneal tissue selection before penetrating keratoplasty. *Br J Ophthalmol.* **82**, 382 - 388 (1998).
27. Borderie, V.M., Baudrimont, M., Lopez, M., Carvajal, S., Laroche, L. Evaluation of the deswelling period in dextran-containing medium after corneal organ culture. *Cornea.* **16**, 215 - 223 (1997).
28. LL Tech. *Light-CT Scanner.* http://www.lltechimaging.com/products-applications/products/ (2017).
29. Doughty, M.J., Müller, A., Zaman, M.L. Assessment of the reliability of human corneal endothelial cell-density estimates using a noncontact specular microscope. *Cornea.* **19**, 148 - 158 (2000).
30. Irsch, K., Borderie, M., Grieve, K., Plamann, K., Laroche, L., Borderie, V.M. Objective analysis of stromal light backscattering with full-field optical coherence tomographic microscopy shows potential to quantify corneal transparency. *Frontiers in Optics.* OSA Technical Digest (online), paper FW6A.6 (2015).
31. Tisdale, A.S., Spurr-Michaud, S.J., Rodrigues, M., Hackett, J., Krachmer, J., Gipson, I.K. Development of the anchoring structures of the epithelium in rabbit and human fetal corneas. *Invest Ophthalmol Vis Sci.* **29**, 727 - 736 (1998).
32. Karimi, A.H., Wong, A., Bizheva, K. Automated detection and cell density assessment of keratocytes in the human corneal stroma from ultrahigh resolution optical coherence tomograms. *Biomed Opt Express.* **2**, 2905 - 2916 (2011).
33. Ku, J.Y., Niederer, R.L., Patel, D.V., Sherwin, T., McGhee, C.N. Laser scanning in vivo confocal analysis of keratocyte density in keratoconus. *Ophthalmology.* **115**, 845 - 850 (2008).
34. Ozgurhan, E.B., Kara, N., Yildirim, A., Bozkurt, E., Uslu, H., Demirok, A. Evaluation of corneal microstructure in keratoconus: a confocal microscopy study. *Am J Ophthalmol.* **156**, 885 - 893 (2013).
35. Erie, J.C., Patel, S.V., McLaren, J.W., Nau, C.B., Hodge, D.O., Bourne, W.M. Keratocyte density in keratoconus. A confocal microscopy study. *Am J Ophthalmol.* **134**, 689 - 695 (2002).
36. Imre, L., Resch, M., Nagymihaly, A. Konfokale In-vivo-Hornhautmikroskopie nach Keratoplastik. *Ophthalmology.* **102**, 140 - 146 (2005).

37. Niederer, R.L., Perumal, D., Sherwin, T., McGhee, C.N. Laser scanning in vivo confocal microscopy reveals reduced innervation and reduction in cell density in all layers of the keratoconic cornea. *Invest Ophthalmol Vis Sci.* **49**, 2964 - 2970 (2008).
38. Patel, S., McLaren, J., Hodge, D., Bourne, W. Normal human keratocyte density and corneal thickness measurement by using confocal microscopy in vivo. *Invest Ophthalmol Vis Sci.* **42**, 333 - 339 (2001).
39. Komuro, A., Hodge, D.O., Gores, G.J., Bourne, W.M. Cell death during corneal storage at 4 degrees C. *Invest Ophthalmol Vis Sci.* **40**, 2827 - 2832 (1999).
40. Gambato, C., Longhin, E., Catania, A.G., Lazzarini, D., Parrozzani, R., Midena, E. Aging and corneal layers: an in vivo corneal confocal microscopy study. *Graefes Arch Clin Exp Ophthalmol.* **253**, 267 - 275 (2015).

